

NOTES ON BASE

This sheet is one in a series of maps of Venus at nominal scales of 1:50,000,000 and 1:10,000,000. Planetary Cartography Working Group, 1984 and 1993. Barnes and others, 1990. It is based on data from the Magellan Synthetic Aperture Radar (SAR) instrument. The Magellan Mission was described by Saunders and Pettengill (1991). Magellan radar characteristics were described by Pettengill and others (1991).

ADOPTED FIGURE

The figure of Venus used for the construction of the map projection is a sphere with a mean radius of 6,051.8 km, consistent with the preliminary gravity figure reported by Phillips and others (1978) that was used for previous maps of Venus. Slightly larger values of the mean radius of Venus have subsequently been reported based on Pioneer Venus (Pettengill and others, 1988) and Magellan altimetry (Ford and Pettengill, 1992).

PROJECTION

The Mercator projection is used for this sheet. The scale is 1:16,354,349 at 0° latitude, 1 in 19,145,190 at 54.0° latitude, as is the scale at 84 latitude in the polar stereographic projection. Due to the retrograde rotation of Venus, longitude increases from west to east in accordance with usage of the International Astronomical Union (1971).

CONTROL

Planimetric control is derived from the radio-tracked position of the spacecraft. The first meridian passes through the central peak of the crater Anaxares, at lat 43.8° N, according to current International Astronomical Union convention. Slalike regions are feature-free, which, at the same longitude, originally fixed the location of the prime meridian (Debes and others, 1986). The Venusian cartographic coordinate system was described by Debes and others (1990).

MAPPING TECHNIQUES

Magellan SAR data were originally produced by the Jet Propulsion Laboratory. Full resolution (75 m/row) image strips were compressed and resampled to produce COMDEX (Compressed Once Modified Image Data Record, 225 m/row) (Pettengill and others, 1991). COMDEX were assembled and reprojected to produce the map. Cycles 1 and 2 left beam-looking, Cycle 2 and 3 right beam-looking, and Cycle 3 left beam-looking with reduced (steered) incidence angle data records were used in the image mosaic. Cycle 1 radar operations commenced September 15, 1990, and ended May 16, 1991. Cycle 2 began May 16, 1991, and ended January 17, 1992. Cycle 3 began January 17, 1992, and ended September 13, 1992. Geographic processing was done by Robert M. Suchland.

SYNTHETIC APERTURE RADAR (SAR) RANGE INTERPRETATION

Because side-looking radar uses long-wave radiation and an imaging geometry distinct from that of viewing cameras, radar images differ from conventional photographs (Ford and others, 1991, p. 45-56, and Young, 1990, p. 73). These differences should be kept in mind when interpreting radar images. Brightness in radar images is dependent on three factors: topography, surface texture, and surface electrical properties.

Topography affects radar images as it affects photographs. Surfaces sloping toward the source of illumination appear brighter and surfaces sloping away appear darker. However, note that the source of illumination for SAR radar images, the radar beam, is the same as the site of the observation, the receiving antenna (fig. 2). This geometry gives SAR images a different perspective from most photographs, where the illumination source is usually the sun and is independent of the observing position. Radar properties are most effectively seen in SAR images when they are relatively steep. Shallow slopes are not shown well in SAR images.

Surface texture strongly affects radar brightness and may have little effect in photographic images. Surfaces whose roughness is comparable with the radar wavelength (12.6 cm for Magellan; Pettengill and others, 1991) scatter more energy back to the radar receiver than do smooth, mirror-like surfaces, so surfaces composed of very small particles such as sand or silt, which will be transparent to or, if of sufficient depth, absorb radar waves appear dark. Thus, areas that appear dark in a photograph may be bright in a radar image, and vice versa.

The third major influence on radar brightness is due to the electrical properties of the surface materials having higher dielectric constants reflect radar waves more strongly, and hence appear brighter. Iron materials having low dielectric constants. Variations in dielectric constants over most of Venus are subtle, and their influence on image brightness is generally overwhelmed by that of relief or roughness variations. However, brightness is significantly enhanced plant-like for materials at elevations above a radius of about 6,050 km (Diller and others, 1990). The electric properties are dependent on frequency; high reflectivity in the radar images does not necessarily correlate with high reflectivity in the optical part of the spectrum.

The side-looking geometry of imaging radar leads to geometric distortion ("layover") of features with significant relief. Slopes facing the radar appear foreshortened. In extreme cases, where the slope angle exceeds the incidence angle (fig. 2), the radar echo from the base of the slope is received before the echo from the top so that the surface may even appear to be folded back upon itself. Consequently, slopes facing away from the radar appear elongated. The amount of layover increases with decreasing incidence angle; the incidence angle used by Magellan as a function of latitude is shown in figure 3. Gravity-related explanations of these effects, as well as summaries of Magellan operations and mission geology can be found in the Magellan Venus Explorer's Guide (Young and others, 1990) and in the Guide to Magellan Image Interpretation (Ford and others, 1993). The latter is substantially more technical.

NOMENCLATURE

V 10M 30/240 CM: Abbreviation for Venus, 1:10,000,000 series, center of map, lat 30° N, long 240°; controlled mosaic; COMEX

REFERENCES CITED

Barnes, R.M., Kite, R.L., Edwards, K.J., and Morgan, H.F., 1994, Venus cartography, *Journal of Geophysical Research*, v. 99, p. 21,573-21,582.
Debes, M.E., and ten others, 1986, Report of the IAU/SAG-COSPAR Working Group on Cartographic Coordinates and Rotational Elements of the Planets and Satellites, *Celestial Mechanics*, no. 39, p. 103-113.
Debes, M.E., and eight others, 1992, The rotation period, direction of the north pole, and geodetic control network of Venus, *Journal of Geophysical Research*, no. 97, no. 8, p. 13,141-13,152.
Ford, J.F., and seven others, 1993, Guide to Magellan Image Interpretation, Jet Propulsion Laboratory publication 93-24, 148 p.
Ford, J.F., and Pettengill, G.H., 1992, Venus topography and kilometer-scale slopes, *Journal of Geophysical Research*, v. 97, p. 13,109-13,114.
International Astronomical Union, 1971, Commission 56: Physical study of planets and satellites, in *Proceedings of the 14th General Assembly, Brighton, 1970*; Transactions of the International Astronomical Union, v. 14B, p. 128-137.
Pettengill, G.H., and five others, 1989, Pioneer Venus radar results: Altimetry and surface properties, *Journal of Geophysical Research*, v. 85, no. A13, p. 82,261-82,276.
Pettengill, G.H., and five others, 1991, Magellan: Radar performance and data products, *Science*, v. 252, no. 5003, p. 260-265.
Phillips, R.J., and five others, 1979, The gravity field of Venus: A preliminary analysis, *Science*, v. 206, no. 4462, p. 83-86.
Planetary Cartography Working Group (Strom, R.G., and ten others), 1984, Planetary cartography in the next decade (1984-1994), National Aeronautics and Space Administration Special Publication 84-71, 71 p.
Planetary Cartography Working Group (Zandbergen, J.K., and seven others), 1993, Planetary cartography 1993-2003, National Aeronautics and Space Administration Planetary Cartography Working Group, 50 p.
Saunders, R.S., and Pettengill, G.H., 1991, Magellan: Mission summary, *Science*, v. 252, no. 5003, p. 242-249.
Tjan, G.L., Ford, J.F., Campbell, D.B., Blach, C., Pettengill, G.H., and Simpson, R.A., 1991, Magellan: Electrical and physical properties of Venus' surface, *Science*, v. 252, p. 265-278.
Young, Stanley, ed., 1990, The Magellan Venus Explorer's Guide, Jet Propulsion Laboratory publication 90-24, 197 p.

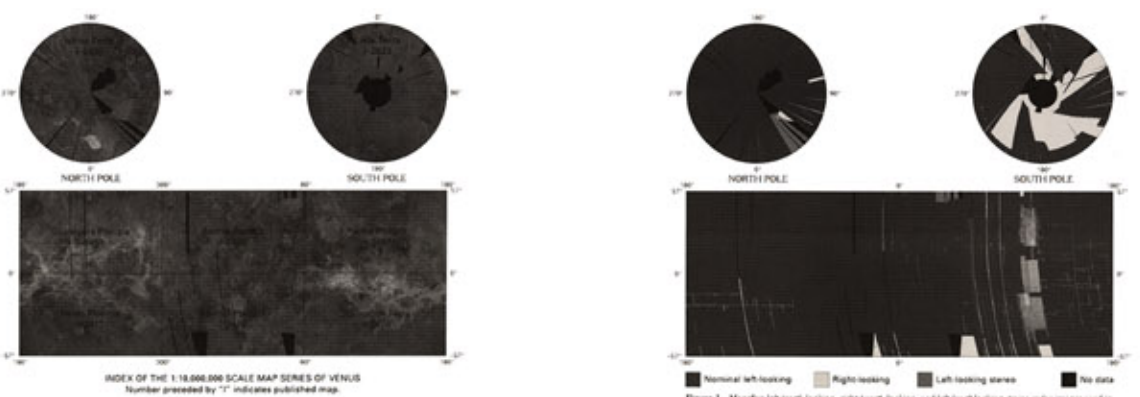
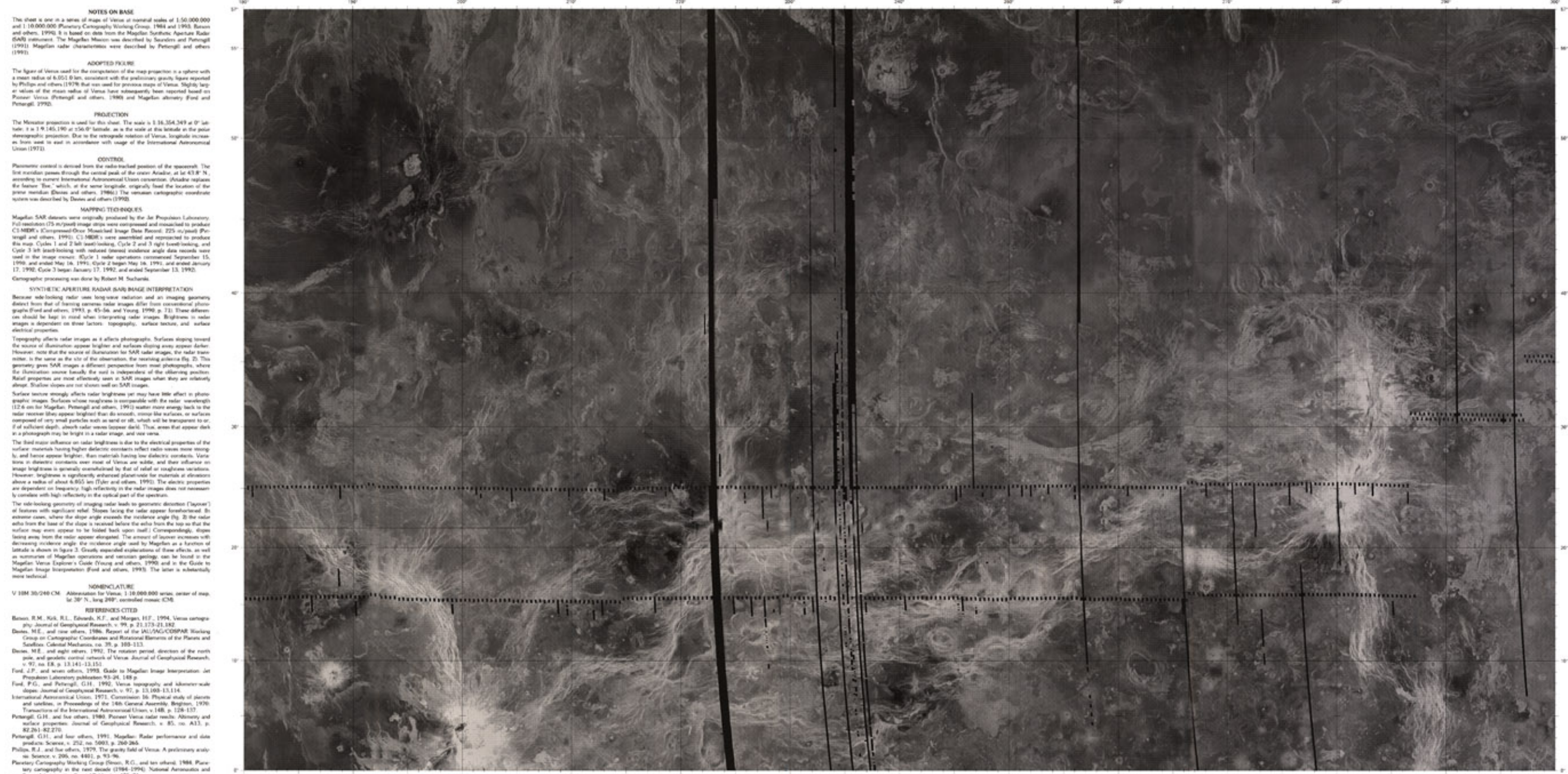


Figure 1. Magellan left beam-looking, right beam-looking, and left beam-looking steered radar images used in the mosaic.

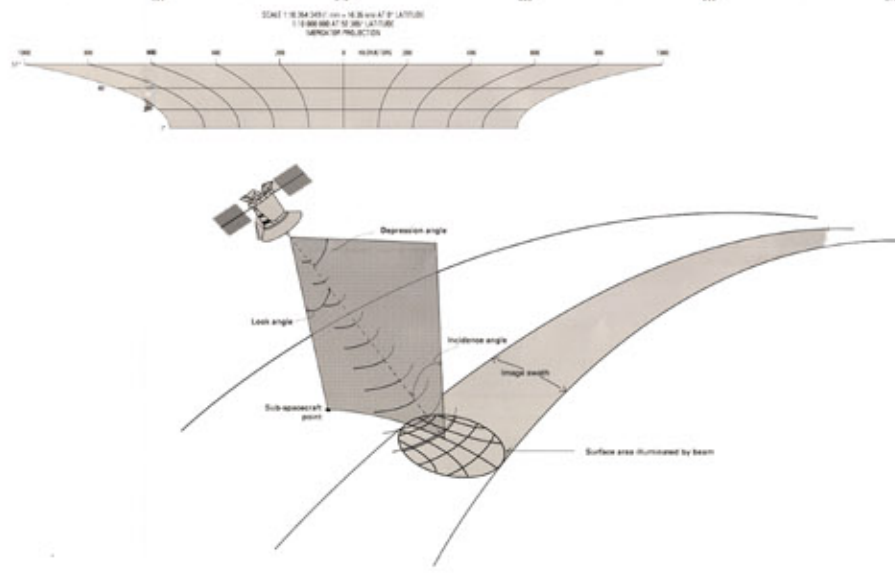


Figure 2. Geometry of the Magellan Synthetic Aperture Radar (SAR) footprint and terminology.

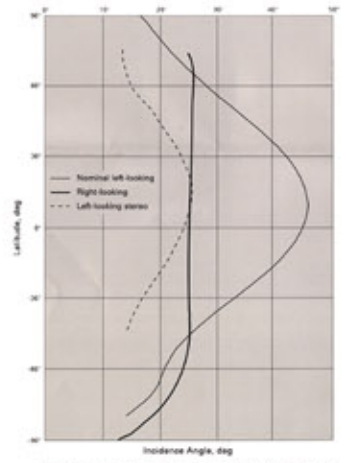


Figure 3. Magellan radar incidence angles as a function of latitude. (Nominal) look angle was varied during right-looking operations to keep the nominal incidence angle at about 25°. Nominal incidence angle was reduced during part of left-looking operations to produce equivalent steering geometry, in combination with nominal left-looking images.

NOTE TO USERS
Users using maps or photocopies are urged to indicate their use of the map or photocopy in the following manner: U.S. Geological Survey, Reston, VA 20192, U.S. Department of the Interior, U.S. Geological Survey, 1-2457 SHEET 1 OF 4.

RADAR IMAGE MAP OF THE GUINEVERE PLANITIA REGION OF VENUS

V 10M 30/240 CM

1998

For sale by U.S. Geological Survey, Information Services, Box 7086, Federal Center, Denver CO 80273

